Time-Resolved Light Scattering Studies on Kinetics of Phase Separation and Phase Dissolution of Polymer Blends.† 1. Kinetics of Phase Separation of a Binary Mixture of Polystyrene and Poly(vinyl methyl ether)

Takeji Hashimoto,* Jiro Kumaki,‡ and Hiromichi Kawai

Department of Polymer Chemistry, Faculty of Engineering, Kyoto University, Kyoto 606, Japan. *Received June 2, 1982*

ABSTRACT: The dynamics of liquid–liquid phase separation of a polymer blend of polystyrene and poly(vinyl methyl ether) was studied by time-resolved elastic light scattering techniques in both the nucleation-growth (NG) and spinodal-decomposition (SD) regimes. It was found that in the early stage of SD the scattered intensity at a given momentum transfer $q = (4\pi/\lambda) \sin(\theta/2)$ increases exponentially with time after the initiation of the isothermal phase separation involved by a temperature jump from the temperature well below the binodal point. The relaxation rate $2R(q)$ of the intensity increase is a function of q such that $R(q)/q^2$ linearly decreases with q^2, in accord with the linear theories of SD originally proposed by Cahn for small molecules and extended by de Gennes for polymers. The spinodal temperature was obtained from the dynamics measured as a function of temperature in the linear SD regime. In the later stage of SD, the intensity increase with time starts to deviate from exponential behavior and the scattering maximum shifts to smaller q, corresponding to the onset of the coarsening process. The higher the superheating, the earlier the stage where the coarsening starts. In the NG regime the intensity increases nonexponentially with time.

I. Introduction

Our objective in this series of studies is to clarify the structure–property relationships of polymer blends in terms of basic molecular parameters such as degrees of polymerization N_A and N_B of polymers A and B, Flory–Huggins interaction parameter χ, Kuhn's statistical segment lengths a_A and a_B, etc. The role of the molecular parameters on the structure and properties is dual, affecting both equilibrium and kinetic aspects of phase separation. That is, they affect mechanisms of the phase separation (nucleation growth (NG) vs. spinodal decomposition (SD)) and the dynamics of the phase separation in the regimes of NG and SD.[1]

Although the equilibrium structure obtained after the phase separation of the mixture is independent of the mechanism of the phase separation but dependent only upon temperature and composition, the intermediate structures developed during the course of phase separation and hence the resulting properties are significantly different for different mechanisms.[1,2] In this regard it is crucial to understand the molecular parameters affecting the mechanism of the phase separation, i.e., the phase boundaries (binodal and spinodal lines[1,3]) for the molecular design of the structure and consequently of the properties.

In order to obtain the intermediate structures one must quench the phase-separated structures at various stages of the phase separation below glass transition temperatures, at a rate much faster than the relaxation rate for the growth of the phase separation. One must therefore know the molecular parameters affecting the dynamics of phase separation. In the event when the processing requires molecular mixing at the processing temperatures, one must know the molecular parameters affecting the binodal temperature and those affecting the dynamics of the phase dissolution.[4] The time required to dissolve the phase-separated structure is a function of the size of the phase-separated domain and the relaxation rate (or the effective diffusivity of molecules) at the processing condition.

In this paper we selected, as a model system, a binary mixture of polystyrene (PS) and poly(vinyl methyl ether) (PVME) having the lower critical solution temperature (LCST) in an appropriate temperature range for the experiments with the time-resolved light scattering technique coupled with a temperature-jump method. Nishi, Wang, and Kwei[5] have already reported some results on thermally induced phase separation behavior of the same polymer blend. They studied the phase diagram and dynamics by using a different approach, i.e., by light transmission, optical microscope, and pulsed NMR methods. Our studies are on the same line as theirs, but we believe that we can obtain more quantitative data by using the light scattering technique, good for quantitative analyses of the mechanisms and dynamics of the thermally induced phase separation, as will be clarified in following discussions.

We will describe results on time-resolved light scattering experiments in section III. We will show that the initial stage of the spinodal decomposition (SD) can be adequately described by the linear theory of Cahn[6] and that modified by de Gennes[7] for polymeric systems. Furthermore from the dynamics of the linear SD regime we will estimate the spinodal temperature as well as some characteristic parameters describing the dynamics. These will be discussed in section IV. Section II will be devoted to brief reviews of the linear theories of the SD. In section IV we shall also discuss the difference in the scattering behavior in SD regime and nucleation-growth (NG) regime (Figure 8). Finally in section V we shall briefly discuss the later stage of SD.

II. Theoretical Background

Cahn and Hilliard[8] described the free energy F of an inhomogeneous binary mixture composed of small molecules (e.g., A and B) in the incompressible limit as

$$F = \int dv \, [f(c) + \kappa(\nabla c)^2 + ...] \qquad \text{(II-1)}$$

where $f(c)$ is free energy density of the system having composition c of one component (e.g., A) which is uniform everywhere in space and the second term is the excess free energy arising from a concentration gradient. The quantity

† Presented in part before 30th annual symposium of Polymer Science, Society of Polymer Science, Japan, Oct 1981. Kumaki, J.; Hashimoto, T.; Kawai, H. *Polym. Prepr., Jpn.* 1981, *30*, 2102–2105.

‡ Present address: Pioneering Research and Development Laboratories, Toray Industries Inc. Co., Sonoyama, Ohtsu, Shiga 520, Japan.

0024-9297/83/2216-0641$01.50/0

c refers to volume fraction of one of the components. By taking the variational derivative of eq II-1, one obtains ($\mu_A - \mu_B$), the chemical potential difference. The flux of each component (J_A or J_B) is then obtained from $D_c(\mu_A - \mu_B)$. An application of the continuity equation $\partial c/\partial t = -\text{div}\, J_A$ to J_A results in the diffusion equation given by

$$\partial c/\partial t = D_c(\partial^2 f/\partial c^2)\nabla^2 c - 2D_c\kappa\nabla^4 c + \ldots \quad \text{(II-2)}$$

where D_c is the translational diffusion coefficient of molecules.

The solution of eq II-2 is obtained by

$$c(\mathbf{r}) - c_0 = \sum_{\mathbf{q}} \exp[R(\mathbf{q})t]\{A(\mathbf{q}) \cos(\mathbf{q}\cdot\mathbf{r}) + B(\mathbf{q}) \sin(\mathbf{q}\cdot\mathbf{r})\} \quad \text{(II-3)}$$

$$R(q) = D_c q^2\{-(\partial^2 f/\partial c^2) - 2\kappa q^2\} \quad \text{(II-4)}$$

where $q = 2\pi/\Lambda$ is the wavenumber of the spatial composition fluctuations and Λ is the corresponding wavelength. The fluctuation $\Delta c(\mathbf{r}) = c(\mathbf{r}) - c_0$ is assumed to be isotropic so that $A(\mathbf{q}) = A(q)$, $B(\mathbf{q}) = B(q)$, and $R(\mathbf{q}) = R(q)$. Equation II-4 was obtained by neglecting the higher order terms of eq II-1 or II-2. We shall call hereafter the theory based upon the linearization approximation as "linear theory" for the sake of convenience. One can calculate the change of elastic scattered intensity with time from eq II-3,

$$I(q, t) \sim \mathcal{F}\{\Delta\tilde{c}(\mathbf{r})\} = I(q, t = 0) \exp[2R(q)t] \quad \text{(II-5)}$$

where q is the magnitude of the scattering vector $\mathbf{q}$, i.e., the momentum transfer vector,

$$q = (4\pi/\lambda) \sin(\theta/2) \quad \text{(II-6)}$$

$\mathcal{F}$ designates a Fourier transform, $\Delta\tilde{c}(\mathbf{r})$ is an autocorrelation function or self-convolution of the function $\Delta c(\mathbf{r})$, λ is the wavelength of light, and θ is the scattering angle in the medium.

In the NG regime, $\partial^2 f/\partial c^2$ is positive (the mixture being stable for the infinitesimal fluctuations), leading to negative $R(q)$ (since κ is positive). Consequently the infinitesimal fluctuations cannot grow but rather can disappear. In the SD regime, $\partial^2 f/\partial c^2$ is negative (the mixture being unstable for the infinitesimal fluctuations), and hence $R(q)$ can be positive for the value of q smaller than the critical $q(q_c)$. Consequently any infinitesimal fluctuations (in amplitude) with the wavenumber $q \leq q_c$ can grow, the relaxation rate of which is given by $R(q)$.[6,8,9]

The linear theory can predict the wavenumber q_m of the spatial composition fluctuations that grow most rapidly in the SD regime and the maximum relaxation rate $R(q_m)$. From eq II-4, it follows that

$$q_m^2 = q_c^2/2 = -(\partial^2 f/\partial c^2)/4\kappa \quad \text{(II-7)}$$

$$R(q_m) = -D_c(\partial^2 f/\partial c^2)/8\kappa \quad \text{(II-8)}$$

It should be noted that q_m is controlled only by *thermodynamics* while $R(q_m)$ is controlled also by the *transport property* D_c. At the spinodal point $T = T_s$,

$$(\partial^2 f/\partial c^2)_{T=T_s} = 0 \quad \text{(II-9)}$$

Consequently

$$q_m^2 = R(q_m) = 0 \quad \text{(II-10)}$$

At $q \ll q_m$, $R(q)$ is dominantly controlled by diffusion, the contribution of which is such that the greater the q the larger the $R(q)$ (i.e., $R_{\text{diffusion}}(q) \sim q^2 D_c$). On the other hand at ($q_c >$) $q \gg q_m$, $R(q)$ is dominantly controlled by thermodynamics, the contribution of which is such that the greater the q, the larger the gradient free energy term and hence the smaller the $R(q)$ (i.e., $R_{\text{thermodynamics}}(q) \sim [-(\partial^2 f/\partial c^2) - 2\kappa q^2]$). Consequently q_m and $R(q_m)$ are determined by a balance of these two physical factors.

The relaxation rate $R(q)$ can be experimentally measured by the time dependence of the elastic scattered intensity of light, X-rays, and neutrons at various reduced scattering angles q accompanied by the phase separation. The existence of $q_m = 2\pi/\Lambda_m$ (wavelength of the spatial fluctuation having maximum relaxate rate $R(q_m)$) and $R(q_m)$ predicts the existence of the scattering maximum at the scattering angle θ_m. The sharpness of the scattering maximum depends on the curvature of $R(q)$ at q_m, i.e.,

$$\left.\frac{\partial^2 R(q)}{\partial q^2}\right|_{q=q_m} = -8D_c\left(\frac{\partial^2 f}{\partial c^2}\right) \equiv 8D_{\text{app}} \quad \text{(II-11)}$$

where D_{app} is "apparent diffusivity", which is efficiently estimated by obtaining an intercept at $q^2 = 0$ in the plot of $R(q)/q^2$ vs. q^2 (see eq II-4).

Consequently it is clear that the dynamics in the linear SD regime is determined by D_c, $-(\partial^2 f/\partial c^2)$, and κ. In order to understand the molecular parameters affecting $-(\partial^2 f/\partial c^2)$ and κ, one needs a specific model relevant to polymer blends. Recently de Gennes[7] proposed a theory of SD for incompressible, binary liquids composed of macromolecules (e.g., A and B) in the context of mean-field approximation. The free energy per lattice site $\tilde{F}$ is given by

$$\tilde{F}/k_B T = (1/N)[c \ln c + (1 - c) \ln(1 - c)] + \chi c(1 - c) + [a^2/(36c(1 - c))](\nabla c)^2 + \ldots \quad \text{(II-12)}$$

where N is the degree of polymerization of A and B polymers (assumed to be $N = N_A = N_B$), and a is the Kuhn statistical segment length (again assumed to be $a = a_A = a_B$). The first two terms of right-hand side of eq II-12 is the free energy corresponding to a uniform mixture given by Flory–Huggins[10,11] and the third term is associated with the composition gradient term including only the "entropic effects" of local variation in c. This entropic effect apparently arises from "connectivity" of monomeric units and therefore is inherent only to polymeric systems. There is also an energetic contribution (to the gradient term), as in eq II-1, associated with the finite range of energetic interactions of monomeric units.[8,12] The energetic contribution is generally small compared with the entropic contribution.[7,13]

Starting from eq II-12, one can derive the relaxation rate for the growth of fluctuations in the linear SD regime:[7]

$$R(q) = q^2\Lambda(q)\left\{2\chi - \frac{1}{Nc(1 - c)} - \frac{a^2q^2}{36c(c - 1)}\right\} \quad \text{(II-13)}$$

where $\Lambda(q)$ is the Onsager coefficient, which is given by

$$\Lambda(q) = Nc(1 - c)D_c \quad \text{(II-14)}$$

for the small q limit,[26] i.e., for the case where SD is achieved by translational diffusion of polymer molecules A and B through the "reptation" process,[14] D_c is the self-diffusion coefficient for translational diffusion of polymers, which is predicted[14] to scale as N^{-2}. Thus from eq II-13 and II-14, it follows that

$$R(q) = q^2 D_c\left[\left(\frac{\chi - \chi_s}{\chi_s}\right) - \left(\frac{R_0^2}{36}\right)q^2\right] \quad \text{(II-15)}$$

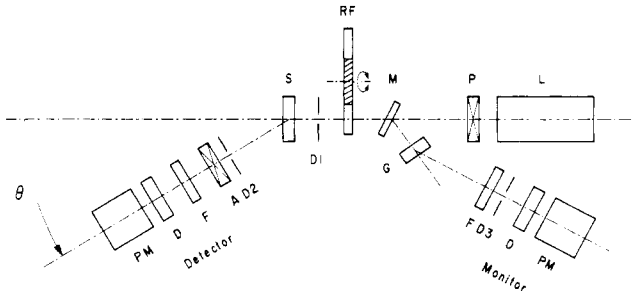

Figure 1. Schematic diagram showing optics of the automated light-scattering photometer.

Consequently $-(\partial^2 f/\partial c^2)$ and κ in the general theory of Cahn are given by

$$-\frac{\partial^2 f}{\partial c^2} = \frac{\chi - \chi_s}{\chi_s} \tag{II-16}$$

$$\kappa = R_0^2/72 \tag{II-17}$$

from which q_m^2 and $R(q_m)$ are obtained. The parameter χ_s is the χ parameter at spinodal temperature

$$\chi_s = [2Nc(1-c)]^{-1} \tag{II-18}$$

and R_0^2 is the unperturbed chain dimension ($R_0^2 = Na^2$). Thus it becomes obvious in the context of mean-field approximation that the molecular parameters affecting the dynamics of the linear SD regime are the degree of polymerization of polymers (N_A, N_B), χ, and the statistical segment length (a_A,a a_B). D_c is a function of N_A and N_B. Thus at a given composition c, the temperature dependence of the dynamics can be predicted if the temperature dependence of χ and D_c is known. In the present status we believe it is very important to pursue critical tests of the theories for various polymer blends.

III. Time-Resolved Light Scattering

1. Specimens. The poly(vinyl methyl ether) (PVME) has number-average molecular weight $\bar{M}_n = 4.6 \times 10^4$ measured by membrane osmometry and heterogeneity index $\bar{M}_w/\bar{M}_n = 2.7$ measured by GPC. Polystyrene (PS) was prepared by anionic polymerization and had the number-average molecular weight $\bar{M}_n = 1.51 \times 10^5$ and $\bar{M}_w/\bar{M}_n = 1.4$. Thin polymer films, about 150 μm, were prepared by casting from 10 wt % toluene solutions of the polymer blend containing 70 vol % PVME and 30 vol % PS, designated as SE-70, where 70 refers to the volume percentage of PVME in the mixture. The toluene solvent cast films, which were reported to be homogeneous,[5,15,16] were further heat treated in a vacuum oven at $T_a = 65$ °C for at least 24 h (T_a is well below the cloud point (97 °C) and well above the glass transition temperature (ca. −25 °C)).

The phase separation was thermally induced by a temperature jump up to temperatures (T_x's) above the binodal point. The temperature jump was achieved by rapidly transferring the specimens at T_a in the heat-treating oven to another chamber controlled at T_x. The time required to achieve the equilibrium temperature T_x is ca. 2 min and T_x is regulated with an accuracy of ±0.1 °C.

2. Light Scattering Photometer. Changes of the scattered intensity distributions with time during the isothermal phase separation were analyzed by an automated laser-light-scattering photometer constructed in our laboratory. The detailed aspects of the apparatus will be described elsewhere.[17] Here we will briefly describe its main part. Figure 1 shows optics of the apparatus. A 20-mW CW He–Ne gas laser was used as an incident light beam and its polarization direction was rotated by polarization rotator P. A part of the incident beam was reflected by a glass slide M, scattered by an opaque glass, and detected by a monitor photomultiplier (PM). The rest of incident beam was passed through a rotating circular neutral density filter (RF) to adjust intensity level of the incident beam and an aperture (D1) to eliminate parasitic scattering from the optics. The scattered beam intensity from the sample (S) was detected by a photomultiplier (PM) through an aperture (D2), which determines the angular resolution of the scattering profile, an analyzer (A), a neutral density filter (F), and an opaque glass (D).

The scanning of the photomultiplier is driven by a pulse motor, the scanning modes being controlled by a microprocessor. The scattered intensity data and the times at which the intensity data are sampled were stored in random access memory (RAM) of the microcomputer. The time data are important since they tell us the time after the isothermal phase separation has been started and also the scattering angles at which the intensity data are sampled during the step-scanning or continuous-scanning operation of PM. The outputs of two PM's are amplified and converted to digitals by 10-bit ADC (analog-to-digital convertor) with 25-μs minimum conversion time and stored in RAM by a program mode with a memory cycle of 18.3 ms. Each intensity datum is an arithmetic average of 20 intensity-data samplings. The scanning rate of the goniometer was 0.66°/s. The input intensity level of the PM was controlled by rotating RF driven with another pulse motor, which is again controlled by software through a driver control and a motor drive. The circular filter RF is such a device that the transmittance varies continuously with its rotation over many decades.

3. Results. Figure 2a shows typical results of data sampling of scattered intensity as a function of time after initiation of the isothermal phase separation of the mixture SE-30 containing 30 vol % PVME in PS at 130 °C under V_v polarization conditions. The PM is scanned back and forth from large θ to small θ and vice versa with time so that the intensity modulates with time as shown in the figure. One can reduce the variation of intensity with time at a given θ as well as the scattering intensity profile with θ at a given time slice, as shown in Figure 2b.

Figures 3 and 4 show the variation of the scattering profiles ($I(q)$ vs. q) with time after the initiation of the phase separation at two temperatures 99.7 and 101 °C, respectively, the spinodal temperature T_s being 99.2 °C as will be discussed in detail in section IV. At each temperature the scattered intensity increases with time at a rate depending on the reduced scattering angle q. After a certain period of time a distinct scattering maximum appears, with its peak position shifting toward smaller q and its peak intensity further increasing with time. The increase of intensity with time is believed to be a consequence of the phase separation according to the SD mechanism, i.e., periodic spatial composition fluctuations being built up. The amplitude $\Delta c(\mathbf{r};q)$ and the wavelength $\Lambda = 2\pi/q$ of the spatial composition fluctuations generally increase with time. The increase of the wavelength is especially remarkable in the later stage of the SD, resulting eventually in the macroscopic phase separation.

The rate at which the intensity profiles change, and hence the kinetics of the phase separation, is dramatically increased by a slight increase of the phase-separation temperature T_x. This increase is primarily associated with an increase of thermodynamic driving force for the phase separation, which, in the context of the linear theory, is given by $(-\partial^2 f/\partial c^2)/\kappa$ in eq II-8 or by $(\chi - \chi_s)^2/\chi_s^2$ in eq II-15 to II-17.[28] In the next section it will be shown that the linear SD theory applies only in the initial stage of the decomposition, as long as about 25 min at 99.7 °C and 10 min at 101 °C. The greater the thermodynamic driving force (or the superheating ΔT), the earlier the stage where the dynamics starts to deviate from that predicted by the linear theory.

IV. Initial Stage of Spinodal Decomposition

Figure 5 shows change of the scattered intensity with time at various q's for SE-70 at 99.7 °C. In the initial stage of the phase separation, the intensity varies exponentially with time at a rate depending upon the reduced scattering angle q and hence the wavenumber q of the spatial composition fluctuations. The exponential increase of the intensity can be described by a linear theory (see eq II-5). The intensity increase with time starts to deviate from that expected from the linear theory in the later stage. The larger the q values, the earlier the stage where the deviations start, e.g., about 20 and 30 min after the initiation of phase separation at $q = 9.2 \times 10^4$ and 4.0×10^4 cm^{-1},

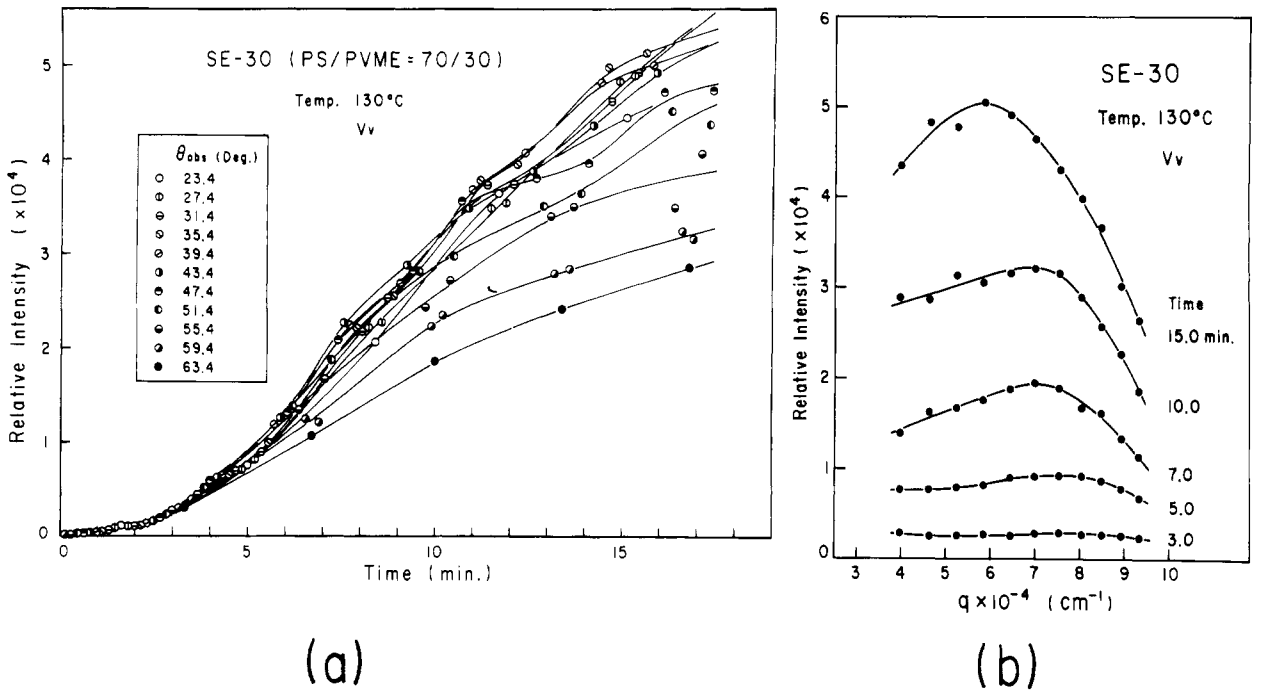

Figure 2. Typical scattering data obtained by the time-resolved scattering technique with the automated photometer for SE-30 at 130 °C under V_v polarization during the course of SD. (a) The scattered intensity as a function of time at various scattering angles and (b) the scattering intensity profiles with the scattering angles at various time slices.

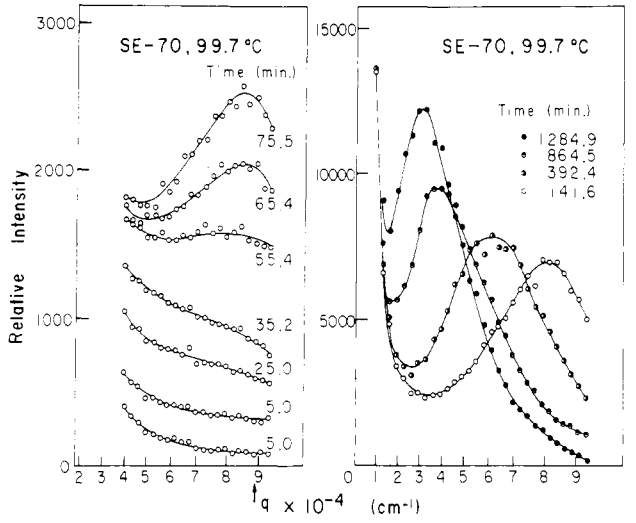

Figure 3. Change of the scattered intensity profiles with time during a course of SD of the polymer blend SE-70 at T_x = 99.7 °C. $q = (4\pi/\lambda) \sin(\theta/2)$. The superheating from the spinodal point T_s, $\Delta T = |T_x - T_s| = 0.5$ °C.

respectively. The deviation is believed to be a consequence of the "coarsening" effect (Ostwald ripening mechanism).[7,18-21] That is, in the later stage the fluctuations become so large that the higher order terms of eq II-1 and II-2 cannot be ignored.

On can estimate the relaxation rate $R(q)$ for the fluctuations to grow as a function of the wavenumber q of the spatial fluctuations from the initial slope of ln $I(q,t)$ in the plot of ln I vs. t, the slope yielding $2R(q)$. The scattering method is superior to the other methods such as pulsed NMR methods as employed by Nishi et al.[5] in that one can analyze $R(q)$ as a function of q and that one can follow, in situ, a rapid growth of the fluctuations without introducing an additional physical process such as freezing a given phase-separated state for the measurements at that state by quenching the specimen below T_g.

Figure 6 shows some results of $R(q)$ as a function of q thus estimated for the SE-70 at 99.7, 100, and 101 °C in the early stage of SD (i.e., in the linear SD region). The maximum relaxation rate $R(q_m)$ increases from ca. 10^{-3} to ca. 4×10^{-3} s^{-1}, and the relaxation time decreases from ca. 1000 to 250 s with a slight increase of temperature by 1.3 °C. In the q range we measured, $R(q)$ increases with increasing q, thus corresponding to the regime where the kinetics are dominantly controlled by the transport phenomenon, i.e., by the term q^2D_c rather than the thermodynamic term in parentheses on the right-hand side of eq II-4.

Figure 7a shows plots of $R(q)/q^2$ vs. q^2 based upon linear theory. A fairly good linear relationship was experimentally obtained, indicating that the early stage of SD for the mixture under investigation can be described by the linear SD theory with good accuracy. From the plots one can estimate the characteristic parameters describing the dynamics of the phase separation such as (i) the "apparent diffusion coefficient" D_{app} from the intercept of $R(q)/q^2$ at $q = 0$, (ii) q_c, the "maximum wavenumber" of fluctuations that can grow from the intercept of q^2 at which $R(q)/q^2 = 0$, or q_m, the "most probable wavenumber" of fluctuations that can grow at the highest rate, q_m being estimated from q_c ($q_m = q_c/2^{1/2}$), and (iii) $R(q_m)$, the "most probably relaxation rate" of the fluctuations. In the context of the mean-field theory, these parameters are given by, from eq II-7, II-8, and II-15 to II-17,

$$D_{app} \equiv \left.\frac{R(q)}{q^2}\right|_{q=0} = D_c\left(\frac{\chi - \chi_s}{\chi_s}\right) \qquad \text{(IV-1)}$$

$$q_m^2 = \tfrac{1}{2}q_c^2 = \frac{18}{R_0^2}\left(\frac{\chi - \chi_s}{\chi_s}\right) \qquad \text{(IV-2)}$$

$$R(q_m)^{1/2} = \frac{3D_c^{1/2}}{R_0}\left(\frac{\chi - \chi_s}{\chi_s}\right) \qquad \text{(IV-3)}$$

From the slope one can estimate

$$|\text{slope}| = 2D_c\kappa = R_0^2D_c/36 \qquad \text{(IV-4)}$$

The parameters thus estimated are summarized in Table I. It is shown that a slight increase of temperature (i.e.,

Table I
Characteristic Parameters Describing Early Stage of Spinodal Decomposition of PVME/PS (70/30 v/v)[a]

temp, °C	q_m,[a] cm^{-1}	q_c,[b] cm^{-1}	Λ_m,[c] Å	Λ_c,[c] Å	$R(q_m)$, s^{-1}	D_{app}, cm^2/s
99.7	9×10^4	1.27×10^5	6.98×10^3	4.94×10^3	1.07×10^{-3}	2.62×10^{-13}
100	9.34×10^4	1.32×10^5	6.72×10^3	4.76×10^3	2.57×10^{-3}	5.85×10^{-13}
101	9.43×10^4	1.33×10^5	6.66×10^3	4.72×10^3	4.23×10^{-3}	9.47×10^{-13}

[a] Data are obtained from the plots of $R(q)/q^2$ vs. q^2 in Figure 7a. [b] $q_c = (2)^{1/2} q_m$. [c] $\Lambda_m = 2\pi/q_m$, $\Lambda_c = 2\pi/q_c$.

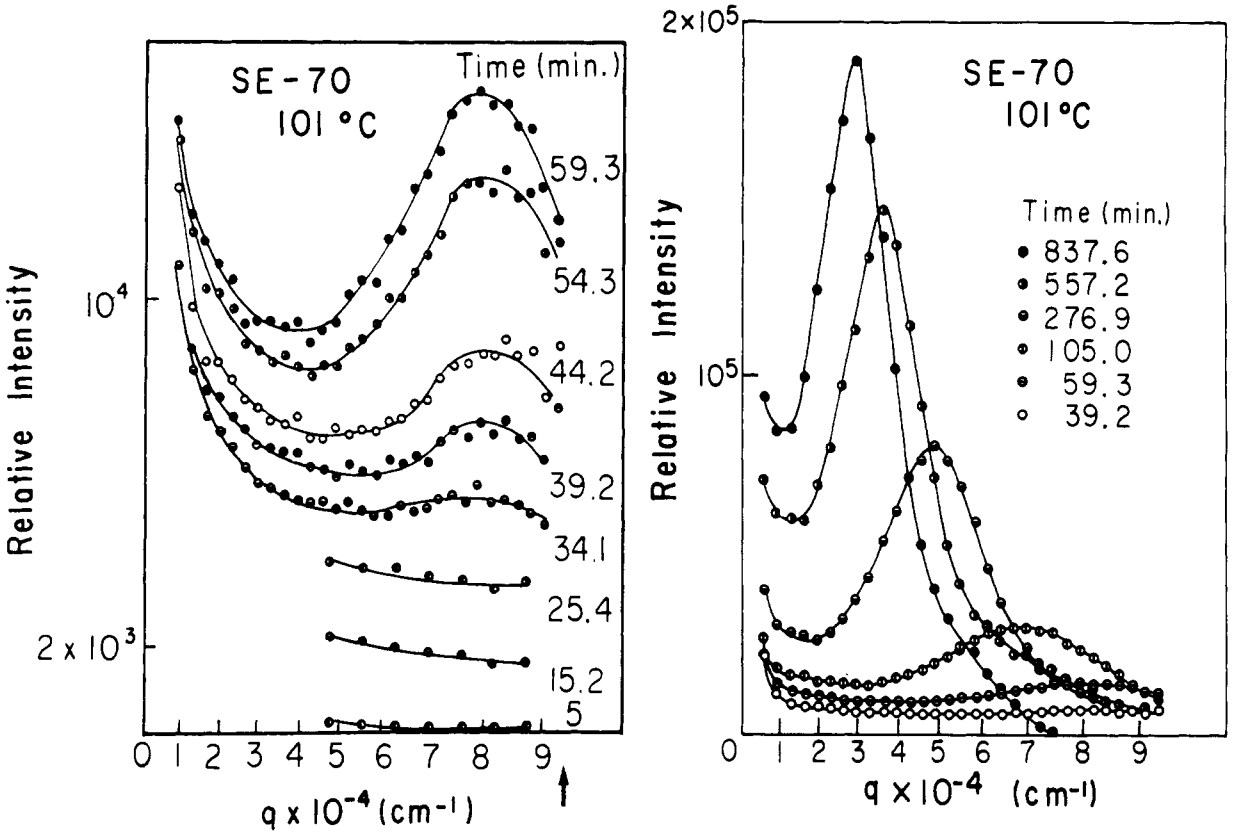

Figure 4. Change of the scattered intensity profiles with time during a course of SD of the polymer blend SE-70 at T_x = 101 °C corresponding to ΔT = 1.8 °C.

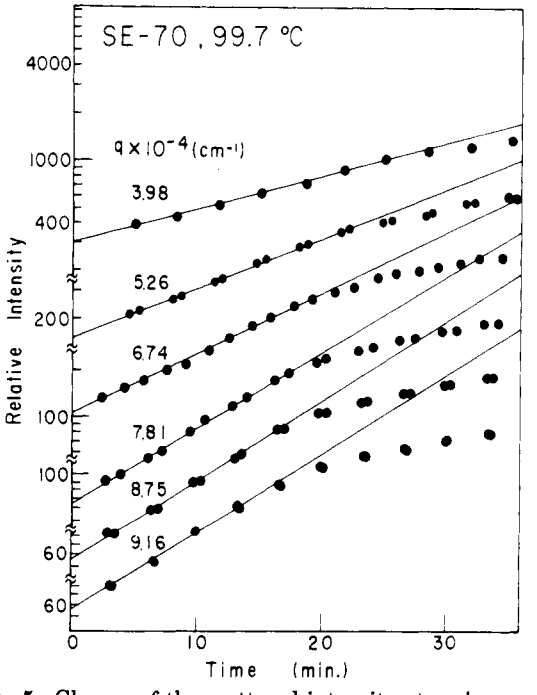

Figure 5. Change of the scattered intensity at various q with time after the initiation of the phase separation at T_x = 99.7 °C for SE-70.

thermodynamic driving force for the phase separation) involves a big change in D_{app} and $R(q_m)$ and a shift of q_m (q_c) and Λ_m (Λ_c) toward larger and smaller values, respectively. These general trends can be qualitatively explained in terms of eq IV-1 to IV-3 by noting that

$$\frac{\chi - \chi_s}{\chi_s} = \frac{1}{\chi_s}\left[\frac{\partial \chi}{\partial T}\right]_{T_s}(T - T_s) + \frac{1}{2\chi_s}\left[\frac{\partial^2 \chi}{\partial T^2}\right]_{T_s}(T - T_s)^2 + \ldots \quad \text{(IV-5)}$$

$$\simeq \frac{1}{\chi_s}\left[\frac{\partial \chi}{\partial T}\right]_{T_s}(T - T_s) \sim (T - T_s) \quad \text{for } T \simeq T_s \quad \text{(IV-6)}$$

The large temperature coefficients of D_{app} and $R(q_m)$ and the large q_m value at a given $\Delta T = (T_x - T_s)$ (compared with other polymer blends such as the polypropylene and EPR (ethylene–propylene rubber) system[22] and ternary systems[23] such as polystyrene (PS), polybutadiene (PB), and toluene and PS, PS-PB diblock polymer, and toluene) suggest that the PS/PVME blend has a large value of $(\partial \ln \chi/\partial T)_{T_s}$ compared with the other systems.

When $T \simeq T_s$, D_{app}, q_m^2, and $R(q_m)^{1/2}$ should linearly increase with T, since D_c and R_0 should not change too much in the narrow temperature range around T_s. At the

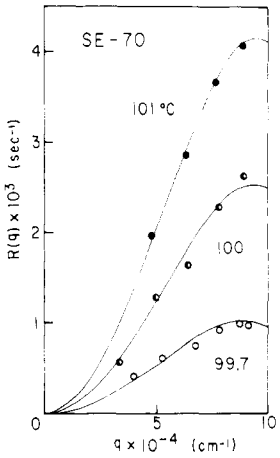

Figure 6. Variation of the relaxation rate $R(q)$ with q for SE-70 at T_x = 99.7, 100, and 101 °C in the linear spinodal decomposition regime.

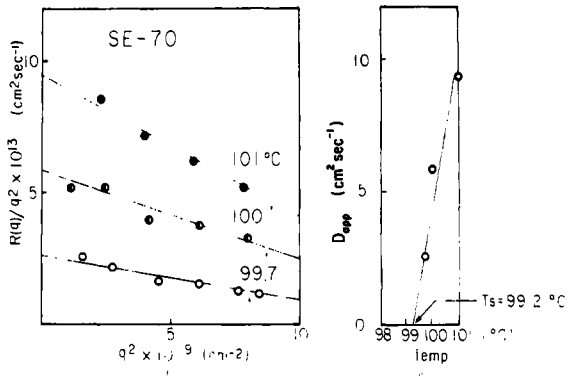

Figure 7. Data analysis in the linear SD regime for SE-70. (a) $R(q)/q^2$ vs. q^2 at three different isothermal phase-separation temperatures T_x, the arrows indicating the positions of q_m^2, and (b) the temperature dependence of $D_{app} = R(q)|q^2|_{q=0}$ from which the spinodal temperature T_s = 99.2 °C is reduced.

spinodal point $T = T_s$, the quantities D_{app}, q_m^2, and $R(q_m)^{1/2}$ vanish.

Figure 7b shows a plot of D_{app} as a function of temperature. A fairly good linear relationship was obtained, from which the spinodal point was estimated to be 99.2 °C. Although the determination of T_s involves some uncertainty, this uncertainty will be reduced by simultaneously observing the intensity change with time at particular q's below and above the estimated T_s as will be discussed later (Figure 8). The slope depends on the characteristic parameters as given by, from eq IV-1 and IV-6,

$$\partial D_{app}/\partial T = 5.5 \times 10^{-13} \text{ cm}^2/\text{s deg} \simeq D_c(T_s)(\partial \ln \chi/\partial T)_{T_s} \quad \text{(IV-7)}$$

The reason the "distinct scattering maximum" is not able to be observed in the linear SD regime is best understood in terms of a small value of $\partial^2 R(q)/\partial q^2|_{q=q_m}$ and hence D_{app} (eq II-11). The arrows in Figures 3 and 4 indicate the position of q_m as estimated from Figure 7a. The systems that exhibit a distinct scattering maximum in the linear SD regime generally have a much greater value of D_{app}, usually 2–3 orders of magnitude greater.[22,23]

It is not well understood at present why the slopes in the plots of Figure 7a depend on the phase-separation temperature T_x. In the context of mean-field theory,[7] the slope should depend on $R_0^2 D_c$ (eq IV-4), which should be almost constant in the narrow temperature range (i.e., 99.7–101 °C). The quantity q_m^2 also starts to deviate from linearity with temperature (as predicted by eq IV-2 and IV-6) at 101 °C, which again is not well understood at present. However we feel we need more quantitative studies on well-fractionated materials for the precise discussions.

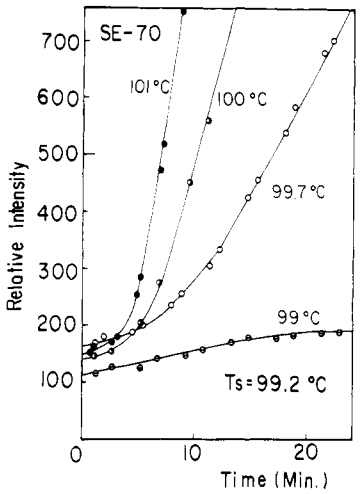

Figure 8. Variation of the scattered intensity at particular q (= 5.6×10^4 cm^{-1}) with time at T_x = 99.7, 100, and 101 °C in the SD regime and at T_x = 99 °C in the NG regime for SE-70.

From the conclusion reduced from Figure 7b, i.e., $T_s \simeq$ 99.2 °C, one can expect that at (T_b <) $T < T_s$ (T_b, binodal point) the phase separation should occur according to the NG mechanism, while at $T > T_s$ it should occur according to the SD mechanism. The difference of the phase-separation mechanisms is spectacularly shown in the difference in the scattered intensity change with time, as shown in Figure 8 for SE-70 at $q = 5.6 \times 10^4$ cm^{-1}. At $T > T_s$ the intensity increases *exponentially* with time, while at $T < T_s$ (e.g., at 99 °C) the intensity increases *nonexponentially* from the beginning of the phase separation, which is considered to be typical of the NG mechanism. The binodal point is believed to be a point where the rate of the nonexponential intensity increase becomes zero.

V. Later Stage of Spinodal Decomposition

In order to obtain parameters characterizing the kinetics of SD over a wide time scale, including both the initial and later stage, we plotted the wavenumber q_m and the peak scattered intensity I_m as a function of time in Figure 9. The borderlines where the kinetics starts to deviate from the linear SD theory and to be affected by the coarsening effect are roughly specified by vertial dash–dot lines. In the linear regime q_m is independent of time and I_m increases exponentially with time in accord with Cahn's theory.[6]

In the later stage q_m starts to decrease with time; thus the characteristic wavelength of the spatial composition fluctuations increase with time, and I_m starts to deviate from the exponential increase with time in such a way that the rate of the intensity increase tends to slow down. As pointed out earlier in section III, at a given thermodynamic driving force $\Delta T = T_x - T_s$ for the phase separation, the deviation starts at an earlier time for the fluctuations with larger q than those with smaller q. If t_c is defined as the critical time where the deviation starts, t_c = 14 and 26 min. for $q = 9.2 \times 10^4$ and 4.0×10^4 cm^{-1}, respectively. At a given q, the higher the value ΔT, the earlier the deviation starts; e.g., at $q = 7.8 \times 10^4$ cm^{-1}, t_c = 17, 9, and 6 min. for T_x = 99.7, 100 and 101 °C (T_s = 99.2 °C).[29]

We will try to fit our results in the later stage with the theories proposed by Langer et al.[21] and Binder et al.[24] as Nojima, Tsutsui, and Nose[25] tried. Langer et al.[21] proposed a theory for the SD in the later stage by taking into account the higher order terms in eq II-1 and II-2. The

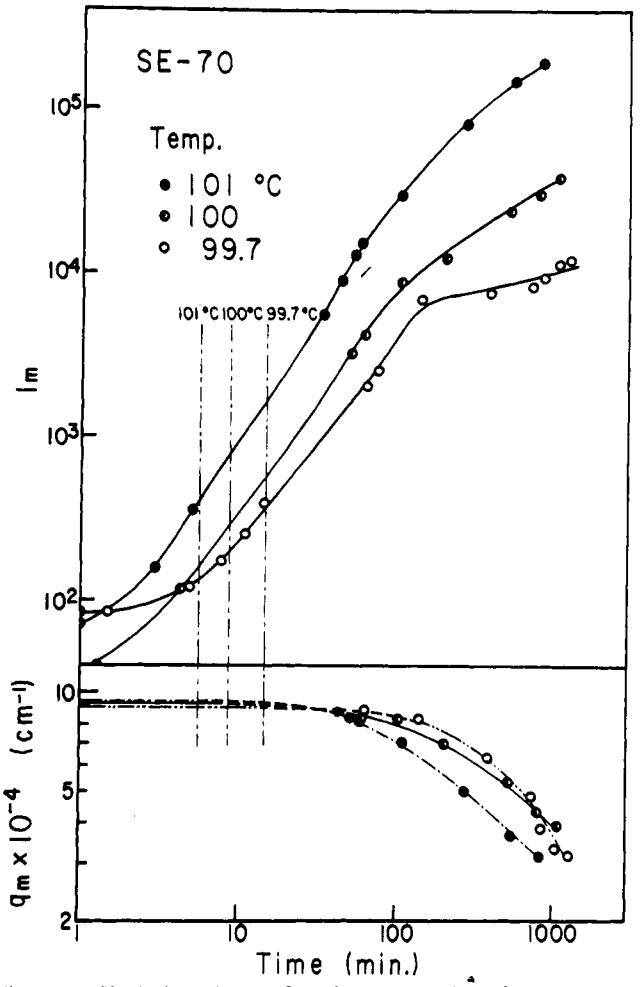

Figure 9. Variation of q_m and peak intensity I_m with time in the early and later stages of SD for SE-70 at T_x = 99.7, 100, and 101 °C.

theory predicts that q_m fits a power-law expression with t,

$$q_m \sim t^{-\alpha} \qquad \alpha = 0.21 \qquad \text{(V-1)}$$

The power-law relationships between q_m and t and between I_m and t were also obtained from the theory of Binder et al. on the basis of cluster dynamics,[24]

$$q_m \sim t^{-\alpha}, \quad \alpha = 1/3; \qquad I_m \sim t^{\beta}, \quad \beta = 1 \qquad \text{(V-2)}$$

Our results in the later stage of SD do not fit too well with the power-law expressions, especially for the smallest ΔT, i.e., the decomposition at 99.7 °C, as in the experimental results reported by Nojima et al.[25] for oligomeric polystyrene and poly(methylphenylsiloxane). The fits of our data I_m and q_m with the power-law expressions yielded the values of α approximately equal to 0.39 and 0.42 at 100 and 101 °C, respectively, and the corresponding values of β approximately equal to 0.8 and 1.1, respectively. The fits of our results with the theories are not generally too good, but the data seem to fit a little better with Binder's theory rather than with Langer's theory.

VI. Concluding Remarks

By using the time-resolved light scattering technique we studied the dynamics of a liquid–liquid phase separation of PS/PVME mixture at a given composition (30/70 v/v) (section III). We have found in the early stage of SD that the intensity increases exponentially with time, with a rate $2R(q)$ of which is a function of the reduced scattering angle q and yields the relaxation rate $R(q)$ for a Fourier component of the composition fluctuations having the wavenumber $q = 2\pi/\Lambda$ (Λ being the wavelength of the fluctuations). The fact of the exponential increase of the scattered intensity with time and the fact that $R(q)/q^2$ linearly decreases with q^2 can predict that the early stage of SD can be described basically by a linear theory proposed by Cahn[6] and modified by de Gennes[7] for polymer blends (section IV). Thus the linear theory can predict the molecular parameters affecting the dynamics (section II).

Our conclusion that the early stage of SD can be described by the linear theory is in accord with the conclusion obtained by Nishi et al.,[5] who showed from the spin–lattice relaxation time T_1 in the pulsed NMR experiments that the total reduction Q of PVME in the PS-rich phase during SD varies exponentially with time in accord with the linear SD theory,

$$Q(t) \equiv \left[\int_{\pi/2q_m}^{3\pi/2q_m} [c(x) - c_0]\, dx\right]^3 \sim \exp[3R(q_m)t] \qquad \text{(VI-1)}$$

The scattering technique is obviously much more powerful than the NMR technique in that one can obtain the relaxate rate $R(q)$ for each Fourier component q of the spatial composition fluctuations as well as the average quantities like $Q(t)$ and $\langle \Delta c^2 \rangle_t$. The assessment of $R(q)$ can allow a critical test such as the linearity of $R(q)/q^2$ and q^2 and the evaluations of the parameters characterizing the dynamics such as D_{app}, q_m, $R(q_m)$, and T_s from the scattering method alone (sections II and IV). Nishi et al.[5] obtained the parameter $R(q_m)$ from NMR measurement on the sample decomposed at a given temperature for a given time duration followed by quenching and the parameter q_m from the microscopic observations. They reduced other characteristic parameters as obtained in this paper from $R(q_m)$ and q_m. The parameters estimated by them are qualitatively in good agreement with ours.

We pointed out, however, that the linear SD theory can describe only the early stage of SD, only a minor fraction of the entire spectrum in the kinetics of phase separation (sections III and IV). The coarsening effect (or Ostwald ripening process) soon appears during the course of SD, resulting in the intensity increase with time, which departs from the exponential increase. The departures are found to start at an earlier stage for greater "superheating" $T_x = T - T_s$ (for the LCST system) at a given q and for larger q at a given T (section V). We found that the functional fits with the power laws (V-1 and V-2) are not generally good. However a better fit was obtained with Binder's theory[24] compared with Langer's theory.[21] From a viewpoint of molecular design of structure and properties we believe it is crucial to understand molecular parameters affecting the later stage of SD.

Finally we should point out that Nojima, Tsutsumi, and Nose[25] recently reported results of kinetic studies of SD as observed by light scattering on a liquid–liquid mixture of oligomeric PS (M_n = 9000) and poly(methylphenylsiloxane) (PMPS) (M_w = 2800). They claimed that even in the early stage of SD, the kinetics does not fit with the Cahn linear theory but rather that their data fit better with the power laws (see eq V-1 and V-2) as proposed by Langer et al. and Binder et al., in contrast to our conclusion and the conclusion obtained by Nishi et al.[5] Our tentative interpretation to this controversy is such that their blend PS/PMPS has a much lower molecular weight than our PS/PVME and hence much higher diffusivity D_c, higher D_{app}, and higher $R(q_m)$ (see eq IV-1 to IV-3), which in turn, should cause the deviation from linear theory at a much earlier stage than ours, at a given thermodynamic driving force $\Delta T = |T - T_s|$ (eq IV-6).

In order to find the linear SD regime for lower molecular weight species, one might have to observe SD at much

lower ΔT or at a much earlier stage.

Registry No. PS, 9003-53-6; PVME, 9003-09-2.

References and Notes

(1) See, for example: Kwei, T. K.; Wang, T. T. In "Polymer Blends"; Paul, D. R., Newman, S., Eds.; Academic Press: New York, 1978; Vol. 1, Chapter 4.
(2) Cahn, J. W. *Trans. Metall. Soc. AIME* **1968**, *242*, 166.
(3) See, for example: Paul, D. R., ref 1, Chapter 1. Krause, S., ref 1, Chapter 2. Sanchez, I. C., ref 1, Chapter 3.
(4) Hashimoto, T.; Kumaki, J.; Kawai, H. *Macromolecules*, part 2 of this series, submitted for publication.
(5) Nishi, T.; Wang, T. T.; Kwei, T. K. *Macromolecules* **1975**, *8*, 227.
(6) Cahn, J. W. *J. Chem. Phys.* **1965**, *42*, 93.
(7) de Gennes, P.-G. *J. Chem. Phys.* **1980**, *72*, 4756.
(8) Cahn, J. W.; Hilliard, J. E. *J. Chem. Phys.* **1958**, *29*, 258.
(9) Cahn, J. W.; Hilliard, J. E. *J. Chem. Phys.* **1959**, *31*, 688.
(10) Flory, P. "Principles of Polymer Chemistry"; Cornell University Press: Ithaca, NY, 1971; Chapter XII.
(11) Huggins, M. *J. Am. Chem. Soc.* **1942**, *64*, 1712.
(12) Debye, P. *J. Chem. Phys.* **1959**, *31*, 650.
(13) Helfand, E.; Sapse, A. *J. Chem. Phys.* **1975**, *62*, 1327.
(14) de Gennes, P.-G. *J. Chem. Phys.* **1971**, *55*, 572. Doi, M.; Edwards, S. F. *J. Chem. Soc., Faraday Trans. 2* **1978**, *74*, 1789.
(15) Bank, M.; Leffingwell, J.; Thies, C. *Macromolecules* **1971**, *4*, 43; *J. Polym. Sci., Polym. Phys. Ed.* **1972**, *10*, 1097.
(16) Nishi, T.; Kwei, T. K. *Polymer* **1975**, *16*, 285.
(17) Saijo, K.; Tanaka, K.; Suehiro, S.; Hashimoto, T.; Kawai, H., to be submitted for publication.
(18) Lifshitz, I. M.; Slyozov, V. V. *J. Phys. Chem. Solids* **1961**, *19*, 35.
(19) Cahn, J. W. *Acta Metall.* **1966**, *14*, 685.
(20) Langer, J. S. *Ann. Phys. (N.Y.)* **1971**, *65*, 53; *Acta Metall.* **1973**, *21*, 1649.
(21) Langer, J. S.; Bar-on, M.; Miller, H. S. *Phys. Rev. A* **1975**, *11*, 1417.
(22) Hashimoto, T.; Tanaka, K.; Kawai, H., to be submitted for publication.
(23) Hashimoto, T.; Sasaki, K.; Kawai, H., to be submitted for publication.
(24) Binder, K.; Stauffer, D. *Phys. Rev. Lett.* **1974**, *33*, 1006.
(25) Nojima, S.; Tsutsumi, K.; Nose, T. *Polym. J.* **1982**, *14*, 225.
(26) For larger q limit where $qR_0 \gg 1$, de Gennes' theory predicts that the Onsager coefficient has a q dependence different from eq II-14. The theory has been corrected and extended by Pincus.[27] However our light-scattering data are obviously associated with the fluctuations occurring at a distance scale much larger than the coil size R_0 (i.e., $\Lambda \gg R_0$), hence satisfying $qR_0 \ll 1$. Consequently our discussions would not be modified by the correction put forward by Pincus.
(27) Pincus, P. *J. Chem. Phys.* **1981**, *75*, 1996.
(28) The increase of the rate of change of the intensity profiles may also be attributable to the change in time scale connected with the increase in the diffusion constant. However for the small temperature variation of T_x (typically a few degrees) as we will discuss in this work, the effect of changing the diffusion constant is negligibly small compared with that of changing the thermodynamic driving force.
(29) The borderlines in Figure 9 correspond to the critical time t_c at $q = q_m$.

Structure and Properties of Tapered Block Polymers. 4. "Domain-Boundary Mixing" and "Mixing-in-Domain" Effects on Microdomain Morphology and Linear Dynamic Mechanical Response

Takeji Hashimoto,* Yasuhisa Tsukahara,† Kazuhisa Tachi,‡ and Hiromichi Kawai

Department of Polymer Chemistry, Faculty of Engineering, Kyoto University, Kyoto 606, Japan.

Received July 12, 1982

ABSTRACT: A series of tapered block polymers of styrene–butadiene (S and P series) and styrene–isoprene (K series) were prepared by anionic polymerization, and the effects of composition variation along the main chain in the tapered block polymers on microdomain structure and on linear dynamic mechanical response were investigated. It was found that the effects are generally twofold: (i) enhancement of mixing of unlike segments in the interfacial region ("interphase") between two coexisting microphases ("domains") (i.e., enlargement of the interphase), designated as "domain-boundary" effect, and (ii) enhancement of mixing of unlike segments in the domains (or domain centers), designated as "mixing-in-domain" effect. The domain morphology and linear dynamic mechanical response were found to be predicted in terms of the two effects, the relative contribution being dependent upon the primary chemical structure. The morphological and mechanical behaviors of the ideal block polymer and S series can be predicted in terms of the domain-boundary effect, while those of the P and K series are dominantly affected by the mixing-in-domain effect.

I. Introduction

Zelinski and Childers[1] reported a large degree of control over monomer sequence distribution can be achieved by anionic copolymerization of butadiene and styrene. For example, when mixtures of butadiene and styrene are copolymerized with lithium alkyls in nonpolar hydrocarbon media, block polymers are formed in which the first block is a copolymer rich in butadiene and the second is one rich in polystyrene. An addition of ether such as diethyl ether to the reaction medium results in the block polymer in which styrene and butadiene monomers are more extensively mixed along the chains.[2-7]

In this paper we define "tapered block polymer" as the block polymers in which composition of one component varies along the main chain. The "ideal block polymer" prepared by a sequential polymerization of styrene and butadiene monomers is effectively a special type of tapered block in which the styrene fraction jumps stepwise from unity to zero along the main chain. The ideal random copolymer in which the comonomers follow each other in statistically random fashion along the chain may be regarded as another extreme of the tapered block in that the fraction of one comonomer averaged over many chains is uniform along the main chain. The effects of the monomer

†Present address: Department of Synthetic Chemistry, Faculty of Engineering, Nagoya University, Furo-Cho, Chikusa-ku, Nagoya 464, Japan.
‡Mitsubishi Petrochemical Co., Ltd., No. 1 Toho-cho, Yokkaichi-city, Mie, Japan.

0024-9297/83/2216-0648$01.50/0